COO--2569-4

Chemiluminescence from AlO: Perturbations, Populations, and Vibrational Analysis for the AlO $A^2\Pi - X^2\Sigma^+$ Transition

MASTER

Michael J. Sayers

and

James L. Gole

Department of Chemistry
Massachusetts Institute of Technology
Cambridge, Massachusetts 02139

DISCLAIMER

Abstract

As a complement to an earlier study of the AlO $B^2\Sigma^+ - X^2\Sigma^+$ emission system, the $A^2\Pi_i - X^2\Sigma^+$ chemiluminescence resulting from the reaction $Al + O_3 \rightarrow AlO^* + O_2$ has been investigated. It is found that the constants extracted for the $A^2\Pi_i$ state by McDonald and Innes adequately describe the vibrational structure of this state to high ($\sim$29) vibrational levels, the behavior being indicative of a Morse oscillator. Perturbations previously observed in the $X^2\Sigma^+$ state are explicitly analyzed in terms of $A^2\Pi_{1/2} - X^2\Sigma^+$ spin-orbit interactions, and a comparison with $A^2\Pi_{1/2} - B^2\Sigma^+$ perturbations is made. Approximate populations $N_{v'}$ for the $A^2\Pi_i$ vibrational levels are determined; the population distribution is dramatically non-Boltzmann, peaking at an energy just below that corresponding to the v=0 level of the $B^2\Sigma^+$ state. This peaking is explained in terms of efficient collisional transfer from the A state to the B state.

I. Introduction

Although the AlO molecule has been studied under a large array of conditions for several years, the understanding of the bonding and kinetic properties of this radical species and its relatives remains incomplete. In an effort to at least partially clarify this situation, several research groups have engaged in single- and multiple- collision chemiluminescence studies of gas phase aluminum oxidation.[1-7] In this paper, we examine the multiple collision reaction of aluminum with ozone, focusing on the low lying $A^2\Pi_i$ state of AlO produced in this metathesis.

Aluminum monoxide is of interest for a number of reasons. Perhaps chief among these is the chemiluminescence and sunlit fluorescence observed when organoaluminum compounds are burned or aluminized grenades are exploded during twilight hours in the upper atmosphere.[8,9] That AlO is present, has been demonstrated by observation of the AlO $B^2\Sigma^+ - X^2\Sigma^+$ emission when solar radiation is present to pump the B state.[9] The radiation from nighttime clouds is observed to consist of a continuous emission peaking at 6300 Å. Despite considerable speculation,[1-7] the relationship between AlO, its relatives, and the continuous emission has remained a mystery ; nevertheless, chemical intuition at least suggests that the AlO species may well have a vital role to play as the emitter, or as an intermediate in the formation of the emitter. The aluminum - ozone reaction under single collision conditions is characterized by an emission continuum[6] on which is superimposed the AlO $B^2\Sigma^+ - X^2\Sigma^+$ band system. Kolb et al.[1] suggested that this continuum and that observed in night releases of TMA (trimethyaluminum) should be associated with highly rotationally excited aluminum oxide emission from the $A^2\Pi_i$ state and possibly quartet ($^4\Sigma$, $^4\Pi$) states populated in an appropriate

reaction.[1] Quite recently, Fontijn[2] has investigated addition and abstraction reactions involving AlO. Although the radiative recombination

$$AlO + O \rightarrow AlO_2^* \qquad (1)$$

$$AlO_2^* \rightarrow AlO_2 + h\nu \qquad (2)$$

is thought to be a rather unlikely process[10], it is suggested as the most reasonable source of the observed upper atmospheric continuum in agreement with an originally postulated mechanism.[11,12] Some very new information[3] suggests that the continuum may result, at least in part, from the hydration of aluminum metal, the emitter corresponding to a polyatomic whose spectrum originates from populated and densely packed rovibronic levels of an excited electronic state.

In addition to its interest as a purely gas phase species, Flödstrom et al.[13] have observed the formation of an AlO layer prior to surface penetration and Al_2O_3 formation during the oxidation of aluminum. Given a more precise elucidation of the gas phase process, one might have a remarkable opportunity to compare directly the reaction dynamics of the gas phase "simple" system, and the chemical interactions characterizing the surface chemistry.

Of course, the AlO $A^2\Pi_i$ state is of interest simply because it is a very low-lying electronic state.[14] In addition, it is the ground electronic state at internuclear distances $R > 1.8$ Å. Since such states are readily populated in the course of many chemical reactions, one expects observable relationships between these states and the chemistry of those systems studied. As an example, recent "multiple collision" studies of the aluminum-ozone reaction[4] have demonstrated the presence of vibrational population anomalies in the $B^2\Sigma^+$ state of AlO. It appears that these local population maxima are the result of strong perturbations between the $A^2\Pi_i$ and $B^2\Sigma^+$ states. It has been postulated that the A state is preferentially populated during formation

of the molecule and that the strong perturbations give rise to "super-highways"[15] allowing extremely efficient collisional transfer to the $B^2\Sigma^+$ state. As will be emphasized in sections III and IV, this mechanism is supported by the results of the present study.

In summary, the $A^2\Pi_i$ state of AlO must be of fundamental significance in those processes involving aluminum oxidation. In this vein, one must ascertain its relevance to the oxidation phenomena. When considering upper atmospheric phenomena, one might ask whether population of the $A^2\Pi$ state represents a significant step in the initial formation of AlO from trimethyl-aluminum and whether or not this state represents an important link in the chain for activation and depletion of the AlO "sunlit fluorescence" seen in the blue-green region of the spectrum. Here, one might comment on our choice of ozone as an oxidant. At the altitudes characterizing upper atmopheric studies, ozone is not the major constituent, and observed reactions probably involve monatomic oxygen[16,17] or water[3]. Nevertheless, ozone is a useful laboratory oxidant because of its high reaction cross section and consequent high photon yield,[18] which facilitates study of the $A^2\Pi_i - X^2\Sigma^+$ emission spectrum. As we will demonstrate in sections III and IV, there is also reason to believe that the features characterizing the aluminum-ozone reaction are similar to those expected for reaction with N_2O molecules and that the A state is sufficiently low-lying that observed relative vibrational populations in this state do not change markedly for the subgroup of reactions whose exothermicity is sufficient to populate the $B^2\Sigma^+$ state.[19]

II. Experimental

The burner and optical system have been described elsewhere.[4,5] Briefly, the aluminum (Alfa products 99.999%) is evaporated from a resistively heated boron nitride crucible,[20] entrained in an argon carrier (Airco 99.998%), and carried to the reaction zone. Here, it is mixed with ozone produced in a commerical Welsbach ozonizer. Typical operating conditions were: P_{Ar} = 1-5 torr, P_{O_3} = 10 - 100μ; T_{oven} = 1700°K. The chemiluminescence was focused onto the entrance slit of a Spex 1701 one meter grating spectrometer equipped with an S-1 response RCA 7102 photomultiplier tube. The photomultiplier signal was detected with a Keithley 417 fast picoammeter and recorded on a Leeds and Northrup strip chart recorder.

III. Results

A. Appearance of the Spectrum

In Figure 1, we present a rapid scan of the rotationally relaxed chemiluminescent emission from the reaction

$$Al + O_3 \xrightarrow{[Ar]} AlO^* + O_2 \qquad (3)$$

The principal features are the red $A^2\Pi_i - X^2\Sigma^+$ and blue-green $B^2\Sigma^+ - X^2\Sigma^+$ emission systems. We also observe weak emission corresponding to the ultraviolet $C^2\Pi_r - X^2\Sigma^+$ system and some aluminum atomic emission lines at $\simeq$ 3950Å. Because of the nature of the high temperature system used in the present studies, care must be taken to alleviate flame contamination from boron oxides. Although BO and BO_2 emission is observed in the flame when the supply of aluminum runs low or the oxidant concentration becomes excessive, no features from either species appear in the spectra discussed herein.[21] The phototube response distorts the relative intensities of the A-X and B-X systems; therefore, an indication of the phototube response is also presented in Figure 1. It has been claimed[5] that the total $A^2\Pi_i$ photon yield is as much as one hundred times that from the $B^2\Sigma^+$ state.

Figure 2 corresponds to the spectrum obtained for the A-X system. The $A^2\Pi_i$ state was first discovered by McDonald and Innes[22] and the $A^2\Pi_i - X^2\Sigma^+$ system was first observed in chemiluminescence by Rosenwaks *et al.*[5] It consists of heavily overlapped, red degraded bands. The high degree of overlap results from a substantial reaction exothermicity ($\Delta H \simeq 96$ kcals/mole) which gives rise to a rich population including many levels of the A state. The system is characterized by favorable Franck-Condon factors for many overlapping sequences. Schamps[23] has calculated that the change in equilibrium internuclear

distance upon passing from the ground state to the A state is $\Delta r_e \simeq 0.15$Å, a change of approximately 10%. This leads to a broad Franck-Condon parabola with widely distributed off-diagonal elements.[24]

B. Analysis of the $A^2\Pi_i - X^2\Sigma^+$ System

Our first concern in analyzing such a rich system was to insure that AlO was indeed the sole carrier, and in particular that only A-X emission was monitored. It was determined that no emission corresponding to the boron oxides, second order features due to the B-X system, or emission from excited states of the oxygen molecule corresponded to the observed features. Although very unlikely, we investigated emission from excited states of O_2. A priori, there are no constraints preventing formation of the $b^1\Sigma_g^+$ state of the oxygen molecule as opposed to excited states of the bond-forming species.[25]

Our initial purpose in the study of the A state was in large part an effort to extend the accuracy of the vibrational energy expression so as to allow reasonable calculation of the levels at energies comparable with those of the $B^2\Sigma^+$ state. In particular, we hoped to extract values for $\omega_e y_e$. In order to pursue this analysis we related band head positions to band origin positions, considering the 12 rotational branches characterizing a $^2\Pi_i - {}^2\Sigma^+$ transition. On the reasonable supposition that the constants extracted by McDonald and Innes[22] in their rotational and vibrational analyses of the $D^2\Sigma^+ - A^2\Pi_i$ and $^2\Delta_i - A^2\Pi_i$ systems are accurate for low vibrational levels, we estimated the value of the rotational quantum number for those branches forming band heads and thence determined $\nu_o - \nu_{head}$. The separation between the $^2\Pi_{1/2}$ and $^2\Pi_{3/2}$ subbands is $\approx$ 128 cm^{-1}, showing that the $^2\Pi$ state closely follows Hund's case (a) coupling. Each subband has six possible branches whose relative intensities we consider. We summarize those features which should be observed as follows:

$^2\Pi_{3/2}$ component (a) Observed vibrational features dominated by coincidentally overlapping $R_2(J)$ and weaker $^RQ_{21}(J) \approx R_2(J-1)$ branch. (b) weaker features due to $^SR_{21}(J)$ may be observed for reactions characterized by relatively high rotational excitation.

$^2\Pi_{1/2}$ component (a) Observed vibrational features dominated by coincidentally overlapping strong $Q_1(J)$ and weaker $^QR_{12}(J) \approx Q_1(J+1)$ branches. (b) Depending upon the magnitude of rotational excitation, emission features due to $R_1(J)$ branch are observed.

Because the observation of strong features is a direct result of bandhead formation in a given branch, the features we observe in Figure 2 are determined by the nature of bandhead formation in a given subband.

For a molecule which closely follows Hund's case (a) coupling the $^SR_{21}(J)$, $^RQ_{21}(J)$, and $^QR_{12}(J)$ branches are reasonably strong; however, as the molecule tends to case (b), these satellite branches may be expected to weaken considerably.[26] In our analysis, we have considered that two possible features can be observed in each subband. For the Q_1 branch, our calculations indicate $J_{head} \leq 5$ and $\Delta\nu_{Q_1} \approx 2 - 6$ cm^{-1}. Noting $J_{head}(R_1) = 3J_{head}(Q_1)$, we find $\Delta\nu_{R_1} \approx 6\text{-}20$ cm^{-1}. At the resolution of the current experiment (10Å), these band origin-band head separations are indistinguishable, and the Q_1 and R_1 branches of the $^2\Pi_{1/2}$ subband are virtually overlapping. A similar analysis of the $^2\Pi_{3/2}$ subband indicates that the R_2 and $^SR_{12}$ branches are also overlapping within experimental resolution. This overlap is in large part the result of the considerably different internuclear separations and hence rotational constants characterizing the $A^2\Pi$ and $X^2\Sigma^+$ states.

In summary, within the resolution of the present experiment, those branches forming band heads are coincidental within a given subband and the separation

between band origins and band heads is indistinguishable.

In identifying vibrational features, our procedure was to first search out combination differences corresponding to well-characterized ground state vibrational quanta. In this way, we hoped to construct v" progressions which could be extrapolated to v" = 0 and thereby obtain the energy of the emitting level.[27] Although this task proved extremely difficult, one crucial fact arose in the course of the analysis. It became apparent that good agreemnt existed between extrapolated levels and even moderately high (v' = 29) levels predicted by the two constant energy expression derived from McDonald and Innes' analysis. It appears that the $\omega_e y_e$ term is so small that it is negligible below the v' = 29 level. From the experimental uncertainty in the v' = 29 level , we can obtain an upper limit for the absolute value of $\omega_e y_e$.[28] We divide the experimental uncertainty by the cube of this maximum observed quantum number and find $|\omega_e y_e| \leq 15\ cm^{-1}/(29.5)^3 = 5.7 \times 10^{-4}\ cm^{-1}$.

C. Vibrational Populations in $A^2\Pi_i$

At the pressures characterizing the present experiment, an initial approach to the analysis of the population distribution for the $A^2\Pi$ state might involve the supposition of a Boltzmann or near-Boltzmann distribution[5] in the vibrational level population. However, recent "multiple collision" studies[4] of the $B^2\Sigma^+ - X^2\Sigma^+$ emission spectrum which results from the aluminum-ozone reaction cast severe doubt on this assumption. An attempt to fit the spectrum to a vibrational temperature confirmed the probability of a non-Boltzmann distribution. Although it was possible to predict the relative intensities for the bands of a single v" progression, it was not possible to obtain the correct intensity ratios between differing v" progressions. Therefore a distribution characterized by a Boltzmann vibrational temperature seemed extremely unlikely.

Figure 3 corresponds to a calculated spectrum for the $A^2\Pi_{3/2} - X^2\Sigma^+$ band system. Peak intensities were calculated from Franck-Condon factors, assuming equal populations in all v' levels. In order to obtain the Franck-Condon factors potential curves were generated using the RKR method.[29] The emission intensity for a given transition is related to the upper state population by[30]

$$I_{v'v''} \propto R_e(\bar{r}_{v'v''})N_{v'}q_{v'v''}\,\nu^4\,\xi(\nu) \qquad (4)$$

where $I_{v'v''}$ is the intensity; R_e is the square of the electronic transition moment at the value $\bar{r}_{v'v''}$; $\bar{r}_{v'v''}$ is the r-centroid of the transition; $q_{v'v''}$ is the Franck-Condon factor; $N_{v'}$ is the upper state population, ν is the transition frequency and $\xi(\nu)$ is an instrumental response function. Based upon previous studies,[4,31] R_e was taken as constant. For the case of equal populations, the intensity relation (1) reduces to

$$I_{v'v''} \propto q_{v'v''}\,\nu^4\,\xi(\nu) \qquad (5)$$

The calculated spectrum, peaking at $\simeq$ 8000Å is in only moderate agreement with the experimentally observed intensities. The experimental spectrum is shifted to the blue, peaking at approximately 7000-7200Å. This suggests that higher v' levels are populated to a greater extent. The calculated system for the $A^2\Pi_{1/2} - X^2\Sigma^+$ system is virtually identical to that for the $^2\Pi_{3/2}$ component. It is shifted 128 cm^{-1} to the blue. This corresponds to a shift of 80 to 125Å across the spectral region studied and shifts the calculated intensity maximum by no more than 50Å. This shift is negligible compared to other considerations.[3] If we impose the constraint of a Boltzmann distribution in the relationships (1) and (2), the calculated spectrum will be considerably red shifted relative to that in Figure 3. Table I presents Boltzmann factors

for several values of T_{vib}. Even for the unreasonably high value T_{vib} = 10,000K, we find a marked dimunition of intensity for higher v' levels which leads to a much simpler red shifted spectrum than that calculated in Figure 3. Clearly, this is qualitatively incorrect.

We have employed equation (1) to obtain a quantitative description of the relative vibrational populations in the levels of the $A^2\Pi$ state. By estimating $I_{v'v''}$ from the peak height[32,33] at frequency ν and using our calculated Franck-Condon factors, we extracted the results for $N_{v'}$ shown in Figure 4. The results for the $\Omega = 1/2$ and $\Omega = 3/2$ components of the $^2\Pi$ state are quite similar. The points plotted correspond to the mean $N_{v'}$ obtained for the progression of ground state levels, v", to which a given v' level emits. Over the spectral range studied, we observe emission from $A^2\Pi$ vibrational levels v' = 7 - 29. As Figure 3 demonstrates, the number of data points which make up the plotted averages increases for each v' as v' increases. For example, the number of data points for v' = 7 and v' = 8 is one; the number of data points for v' = 11 is three and the number for v' = 14 is five. For levels $v' \geq 16$, the number of available data points doubles to a minimum of eight, leading to a considerable increase in accuracy. Because of the nature of the data, the predicted local maxima at v' = 11 and 14 are extremely unlikely. Indeed, it is unlikely that strong interactions exist between these levels and levels of the ground electronic state. For both components (Ω = 1/2, 3/2), the population appears to increase slowly from v' = 7, rising much more rapidly for $v' \geq 21$ to a maximum at $v' = 24 \pm 1$. The population diminishes at an energy corresponding closely to the onset of the $B^2\Sigma^+$ state. For levels $v' \geq 16$, the deviation for calculated points was $\pm$ 17%.[34]

The results presented in Figure 4 are in surprisingly good agreement for both components; however, they can only be considered as a good semiquantitative estimate of the relative populations. The high degree of overlap in the spectrum

necessitates the use of approximate peak heights rather than peak areas. In addition, a correction factor must be applied to account for emission from other systems[35] underlying the short wavelength region of the spectrum. This is difficult since the $A^2\Pi$ emission feature effectively merges into a continuum in this region (Figures 1 and 2). We have applied a correction which represents an upper bound to the contribution from underlying features.[36] By virtue of the nature of this correction, the $A^2\Pi$ state population distribution may peak at slightly higher v' than that level indicated in Figure 4. The key point is the vast qualitative difference between this result and the Boltzmann distribution proposed[5] in the first identification and analysis of this system.

D. Vibrational Perturbations in the $X^2\Sigma^+$ State

The v" = 9 level of the $X^2\Sigma^+$ state is mildly perturbed. Based upon Tyte and Nicholls' compendium,[37] it is shifted up approximately 8 cm^{-1}. McDonald and Innes[22] have suggested that the $A^2\Pi_i$ state is responsible for ground state perturbations; however, no reference to specific levels or the nature of the interaction has been presented. We would like to make a more specific suggestion regarding the v" = 9 level.

Using the McDonald-Innes [22] and Tyte - Nicholls[37] constants for the $A^2\Pi_i$ and $X^2\Sigma^+$ states, we compute that the v' = 4 level corresponding to the Ω = 1/2 spin orbit component of the $A^2\Pi$ state lies only 12.5 cm^{-1} below the v" = 9 level of the $X^2\Sigma^+$ state. Figure 5 corresponds to the calculated level diagram for a portion of the "unperturbed" $A^2\Pi$ and $X^2\Sigma^+$ potential curves. From these curves it is clear that we expect a strong interaction between the v' = 4 and v" = 9 levels. (The Ω = 3/2, v' = 4 level is 140.5 cm^{-1} below $X^2\Sigma^+$, v" = 9.) The Ω = 1/2 level will interact with the ground $^2\Sigma_{1/2}^+$ state through spin-orbit coupling. This interaction is approximately two orders of magnitude stronger than that resulting from Coriolis mixing of the $A^2\Pi_{3/2}$ and $X^2\Sigma_{1/2}^+$ states[38] and therefore the perturbation interaction with the v" = 9 level is dominated overwhelmingly by the Ω = 1/2 component. This interaction is expected to raise the v" = 9 level and lower the v' = 4, Ω = 1/2 level.

Based on Table 1 in McDonald and Innes' paper we find that the spin orbit splitting for the v = 0, 1, 2, and 3 levels of the $A^2\Pi$ state is 129-130 cm^{-1} whereas that for the v = 4 level is 124 cm^{-1}. Because the spin orbit interaction of the Ω = 1/2 component is so much larger than the Coriolis interaction of the Ω = 3/2 component, the 5 to 6 cm^{-1} difference in the measured value of A_{eff} can be attributed to a downward shift of the Ω = 1/2 component.

This downward shift is comparable to that observed for the v" = 9 level in the $X^2\Sigma^+$ state. If we equate the energy separation for the unperturbed states with the energy levels depicted in Figure 5,[39] the separation between the perturbed levels will be $\Delta\nu \approx 24.5\ cm^{-1}$ ($12.5 + 2 \times 6\ cm^{-1}$). This energy difference can be related to the strength of the perturbation ω, and the energy separation of the unperturbed states, δ. We have[4]

$$\omega = 1/2\{(\Delta\nu)^2 - \delta^2)\}^{1/2} \qquad (6)$$

with $\delta = 12.5\ cm^{-1}$, $\omega = 10.54\ cm^{-1}$.

The calculated quantity, ω, can be expressed as the product of an electronic plus rotational component and a vibrational overlap. This vibrational overlap for the v' = 4, v" = 9 levels, obtained from calculated RKR curves, is 0.3432 and therefore

$$\omega \sim 30.7 \langle v'|v''\rangle \qquad (7)$$

This interaction should be compared with the semiempirical value[4]

$$\omega \sim 86 \langle v|v'\rangle \qquad (8)$$

found for the spin orbit interaction between the $A^2\Pi$ and $B^2\Sigma^+$ states of AlO. One might ask why the electronic plus rotational component is considerably lower for the $A^2\Pi_{1/2} - X^2\Sigma^+_{1/2}$ interaction. Some insight can be provided by briefly considering the spin-orbit interaction. We have

$$\omega = \langle\Psi_1|H_{so}|\Psi_2\rangle \qquad (9)$$

where Ψ_1 and Ψ_2 are the wavefunctions for the unperturbed levels and

$$H_{so} = \sum_{i,k,\alpha} \xi_k(r_{ki}) \ell_{ik}^{\alpha} s_i^{\alpha} \qquad (10)$$

where the sum is over electrons i and nuclei k, ℓ_{ik}^{α} and s_i^{α} are the α = x, y, or z components of the orbital and electron spin angular momentum, and $\xi_k(r_{ki})$ is the spin orbit constant proportional to the inverse cube distance, r_{ki}^{-3}, between electron i and nucleus k.[40,4]

The wavefunctions Ψ_1 and Ψ_2 can be evaluated in a manner similar to that used in considering the spin orbit interaction between the A and B states.[4] Because parity is a good quantum number, wavefunctions are written in a parity basis. Linear combinations which transform as eigenfunctions of the parity operator are[4,38]

$$|\pm^{2}\Sigma^{+}_{1/2}, v\rangle = 1/\sqrt{2}\,[|\Lambda = 0, s = 1/2, \Sigma = 1/2\rangle|\Omega = 1/2, J\rangle \pm (-1)^{J-1/2}|\Lambda = 0, s = 1/2, \Sigma = -1/2\rangle|\Omega = -1/2, J\rangle]|v\rangle \tag{11}$$

$$|\pm^{2}\Pi_{1/2}, v\rangle = 1/\sqrt{2}\,[|1, 1/2, -1/2\rangle\,|\,1/2, J\rangle \pm (-1)^{J-1/2}\,|-1, 1/2, 1/2\rangle|-1/2, J\rangle]|v\rangle \tag{12}$$

where both wavefunctions are written as the product of an electronic and vibrational factor, and Λ, Σ, and Ω are the projections of the orbital, electron spin(S), and total angular momentum on the molecular axis. Substituting the expressions (11) and (12) for Ψ_1 and Ψ_2 in equation (9) allows the evaluation of the spin-orbit matrix element. The resulting expression can be simplified by re-expressing the basis functions $|\Lambda S\Sigma\rangle$ in terms of antisymmetrized products of one electron molecular orbitals.[4] The electronic configurations for the $X^2\Sigma^+$, $A^2\Pi$, and $B^2\Sigma^+$ states are respectively:

$$\ldots(2\pi)^4\ (6\sigma)^2\ (7\sigma) \qquad X^2\Sigma^+ \tag{13}$$

$$\ldots(2\pi)^3\ (6\sigma)^2\ (7\sigma)^2 \qquad A^2\Pi \tag{14}$$

$$\ldots(2\pi)^4\ (6\sigma)\ (7\sigma)^2 \qquad B^2\Sigma^+ \tag{15}$$

Considering the interaction between the $A^2\Pi$ and $X^2\Sigma^+$ states and omitting the 6σ orbital which remains doubly occupied in both $X^2\Sigma^+$ and $A^2\Pi$,

$$\begin{aligned} |0\ 1/2\ 1/2\rangle &= |\ A(\ldots\ 1_2^+\ 1_2^- - 1_2^+ - 1_2^-\ 0_7^+)\rangle \\ |1\ 1/2\ -1/2\rangle &= |\ A(\ldots\ 1_2^+\ 1_2^- - 1_2^-\ 0_7^+\ 0_7^-)\rangle \end{aligned} \tag{16}$$

where numerals 0 and $\pm$ 1 identify the z component of the orbital angular momenta, ℓ_i, and superscripts $\pm$ specify the corresponding projection of s_i. A is the antisymmetrizing operator and subscripts 2 and 7 pertain to molecular orbitals 2π and 7σ respectively. In a manner analogous to that discussed in reference 4, we reduce the many electron integrals obtained upon substitution of the expressions (11) and (12) to tractable sums over one-electron integrals arriving at a final expression

$$\omega = 1/2\ \langle v'|v''\rangle\ \langle -1_2|\ \sum_k \xi_k(r_k)\ell_k^-\ |0_7\rangle \tag{17}$$

If we were to replace the 7σ orbital (0_7) in equation (17) with the $6\sigma(0_6)$ orbital, we obtain an expression for the spin orbit interaction between the $B^2\Sigma^+$ and $A^2\Pi$ states upon adjustment of the vibrational overlap factor.

A complete evaluation of ω for either the $A^2\Pi$ - $X^2\Sigma^+$ or $A^2\Pi$- $B^2\Sigma^+$ spin orbit interactions requires some knowledge of the molecular orbitals $|-1_2\rangle = 2\pi$, $|0_6\rangle = 6\sigma$, and $|0_7\rangle = 7\sigma$. It is here that the basic difference in magnitudes for the spin orbit interactions arises. The presence of $\xi_k(r_k) \sim r_k^{-3}$ insures that only one-center integrals will make a significant contribution to

Eq. (17).[41] While the 2π and 6σ orbitals are centered on oxygen for both the $B^2\Sigma^+$ and $A^2\Pi$ states and the molecular orbitals are reasonably represented by atomic p orbitals centered on an oxygen ion (O^-)[4,23], the ground state 7σ orbital is shared between the oxygen and aluminum atoms. Therefore, the "single center" matrix element (17) will be much smaller than that for the $A^2\Pi$ - $B^2\Sigma^+$ interaction. If we make the drastic assumption that the "double zeta + polarization" description of the $X^2\Sigma^+$ state (Al^+O^-) is realistic, we arrive at a calculated interaction[4] (using the population analysis given in ref. 23)

$$\omega = 43 \ \langle v' | v'' \rangle \qquad (18)$$

A more realistic description would involve the shift of more charge density to the oxygen atom, leading to an even smaller interaction term (18).[42]

IV. Discussion

The beam-gas chemiluminescent emission from the "single collision" reaction of aluminum with ozone is characterized by the continuous emission depicted in Figure 6. The "multiple collision" spectrum is inset for comparison. The combined spectra demonstrate the important role of AlO $A^2\Pi$- $X^2\Sigma^+$ emission in the "single collision" continuum. It is apparent that the continuum is characterized by densely packed structure corresponding to emission from numerous rovibronic levels of those excited electronic states produced as the nascent products of reaction. Based upon comparison with the "multiple collision" results, the spectrum appears to correspond to the $B^2\Sigma^+$ - $X^2\Sigma^+$ and $A^2\Pi$ - $X^2\Sigma^+$ band systems of AlO. It is dominated at longer wavelengths by the A-X system whereas the B-X system begins to contribute at wavelengths shorter than 5800 Å. In view of the present results, it appears that the continuous emission observed in the laboratory oxidation of aluminum[5-7] and upon explosion of aluminized grenades or the release of TMA into the upper atmosphere may be due, at least in part, to AlO $A^2\Pi$ - $X^2\Sigma^+$ emission. There are, however, more complications which must be considered in a complete analysis of the laboratory and upper atmospheric emissions.[3]

In the remainder of this discussion we will be concerned with the vibrational population distribution in the A state and its relationship to our previous analysis of the $B^2\Sigma^+$ - $X^2\Sigma^+$ multiple collision emission spectrum.[4] Based upon relative non-Boltzmann vibrational population anomalies in the $B^2\Sigma^+$ state and the possibility of strong "spin orbit" interaction between the A and B states, the Al + O_3 reaction is thought to proceed as follows:[4] The initial step which leads to AlO* formation corresponds to an electron jump

at large internuclear distance and subsequent population of the A and X states. This electron jump distance is sufficiently large (4.1Å) so that the A state is in fact the ground state (Figure 5 - reference 4) and is therefore selectively populated.[43] Following the initial step, collisions with argon atoms induce transitions to B state vibrational levels which interact strongly with high vibrational levels of the A state.

Because the A state potential appears to be Morse-like and can be well represented by an expression involving only the first order anharmonicity correction up to levels v' = 30,[39] we may estimate those high A state levels which interact with the B state. Previously[4], it was felt that extension of the two constant description for the A state was unjustifiable; however, the small value of $\omega_e y_e$ lends validity to the parametrization. Using the constants given by Tyte and Nicholls[37] and those of McDonald and Innes[22], and noting that only the Ω = 1/2 component of $A^2\Pi$ interacts strongly with the B state,[4] we may equate the energies of the A state with the v = 12 and 14 levels of the B state. We have[44]

$$E^B(v=12) = 31017.7\ cm^{-1} \approx 5468.9 + 728.5\ (v+1/2) - 4.15(v+1/2)^2 \quad (19)$$

$$E^B(v=14) = 32568.8\ cm^{-1} \approx 5468.9 + 728.5(v'+1/2) - 4.15(v'+1/2)^2 \quad (20)$$

Solving the expressions (19) and (20), we find v = 48, v' = 53. Direct substitution yields $E^A(48)$ = 31039.1 and $E^A(53)$ = 32565.3. Given a small negative $\omega_e y_e$ term[45], we expect that the v = 48 and 53 levels of the A state will lie slightly to the red of the v = 12 and 14 levels of the B state, in agreement with the observed spectrum.[4]

We have emphasized the A state vibrational distribution in this paper in order to draw a correlation with the previously proposed model for the introduction of vibrational population anomalies in the $B^2\Sigma^+$ state.[4] Were the

distribution in $N_v(A)$ remotely Boltzmann, even a rather high vibrational temperature (T_{vib} = 5000K) would give rise to prohibitively small populations at A state energies corresponding to those levels involved in efficient transfer to the B state ($N_v(5000K) \simeq 1.2 \times 10^{-4} N_o$). Thus the previously proposed model for the observed behavior of B state[4] emission implicitly requires a distribution favoring the population of high vibrational levels in the A state. The present results are in agreement with this requirement.

Rosenwaks et al.[5] claim to have computer synthesized the A-X spectrum of AlO assuming a Boltzmann distribution in the vibrational and rotational stacks, finding T_{rot} = 1800K, T_{vib} = 3500K. Our own findings notwithstanding, this result is suspect for several reasons. The most important of these involves a consideration of the time scales characterizing the multiple collision experiment. It appears that a rotational temperature of 1800K is rather high. Using $T_{trans} \cong$ 300K, d_{AlO} = 4.1Å (the hard sphere diameter)[4], and p = 4 torr, we compute[46] a collision time for AlO with argon τ_c = 36 nanoseconds. This collision time should be compared with the radiative lifetime of the A state. This lifetime has not been measured but we may obtain approximate values for τ_{rad} by noting that:

$$\tau_{rad}(A\text{-}X) \simeq \left|\frac{M_{(B\text{-}X)}}{M_{(A\text{-}X)}}\right|^2 \tau_{rad}\,(B\text{-}X) \qquad (21)$$

where M corresponds to the transition moment. The transition moments have been estimated by Yoshimine et al.[31], while τ_{rad} has been determined by a number of workers. Using the minimal and maximal values obtained for $\tau_{rad}(B\text{-}X)$ generally determined from laser induced fluorescence measurement[47], we obtain the result,

$$500 \leq \frac{\tau_{rad}}{\tau_c} \leq 1000 \qquad (22)$$

Thus an $A^2\Pi$ AlO molecule experiences several hundred collisions before radiating. Because R-T transfer is quite efficient[48], we may expect near equilibration between the rotational modes and the ambient gas (argon). Consequently a value of T_{rot} = 1800K seems abnormally high. In comparison, V-T transfer is rather inefficient, and equilibration might not occur even after several hundred collisions between the ambient carrier gas and the vibrational mode.[49]

Given a knowledge of the time scales which characterize the multiple collision experiment, we are forced to examine the computer fit A-X emission spectrum (Figure 2 - reference 5). It appears that Rosenwaks et al.[5] have assigned considerable intensity to bands characterized by both low Franck-Condon and Boltzmann factors. It seems conceivable that a computational error has occurred and that the fit between the synthetic and experimental spectra which is not spectacular may only reflect an accidental similarity.

Let us now consider the specific nature of the observed vibrational population distribution which characterizes the aluminum-ozone reaction. Based upon previous reports, N_2O and microwave discharged oxygen also react to yield the $A^2\Pi$- $X^2\Sigma^+$ and $B^2\Sigma^+$ - $X^2\Sigma^+$ band systems. It has been noted that the AlO A-X emission from the Al-N_2O reaction shows a great similarity to that from the ozone system.[4,5] We believe that these "multiple collision" results can be explained primarily in terms of collisional transfer from the A to the B state (for those reactions which are sufficiently exothermic to populate the B state). We have already noted (1) that collisional transfer between the A and B states is extremely efficient and can occur at every hard sphere collision[4] and (2) that the $A^2\Pi$ state can undergo between 500 and 1000 collisions before radiating.[50] We suggest that the combination of these two factors leads to the peaking in the $A^2\Pi$ vibrational population distribution characterizing the "multiple collision" Al + O_3 reaction.[50] The peaking effect is

dramatically evident in the spectrum depicted in Figure 6. At the much lower pressures ($10^{-4} \rightarrow 10^{-6}$ torr) characterizing the "single collision" aluminum-ozone reaction, collisional transfer from the A state does not compete with radiative decay. The presence of the A-X emission features at much shorter wavelengths in the single collision spectrum is evident through comparison with the multiple collision results.[51] The single collision spectrum must be characterized by emission from $A^2\Pi$ vibrational levels $v' \geq 29$, as well a population distribution peaking at much higher vibrational quanta than that found for the multiple collision spectrum (Figure 4). Note also that the $A^2\Pi$ - $X^2\Sigma^+$ emission system dominates the single collision spectrum whereas the emission from the $A^2\Pi$ and $B^2\Sigma^+$ states is of comparable intensity in the multiple collision spectrum (Figure 1). These relative intensities again indicate efficient collisional transfer from the A to the B state. Were it not for the B state, we would expect the population distribution for the $A^2\Pi$ state to peak at a vibrational level considerably in excess of $v' = 30$.[52]

While the explanation for the multiple collision $A^2\Pi$ and $B^2\Sigma^+$ vibrational distributions characterizing the Al-N_2O reaction may be somewhat more complicated[4], section IIID demonstrates that the substantial portion of those molecules formed in the $A^2\Pi$ state[5,52] can be collisionally transferred to the $B^2\Sigma^+$ state leading to a spectrum similar to that observed for the Al-O_3 reaction.[53] In summary, we believe that the similarity between the multiple collision A-X emission observed for the Al-N_2O and Al-O_3 reactions can be attributed to extremely efficient $A^2\Pi \rightarrow B^2\Sigma^+$ collisional transfer.[54]

Acknowledgement

It is a pleasure to acknowledge support of this research by the National Science Foundation under Grant GP-43691X and the Energy Research and Development Administration under Grant E-(11-1)-2569. Special thanks go to the Research Corporation whose support allowed us to initiate the beginning phases of this work.

References

1. C.E. Kolb, M.E. Gersh, and D.R. Hershbach, Comb. and Flame 25, 31 (1975)
2. A. Fontijn, "Reactions between AlO_x and O atoms", Aerochem Research Labs - preprint TP351. Also see Aerochem preprint TP 338 for supplementary information
3. S. Oblath and J.L. Gole, "On the Upper Atmospheric Emission Observed upon Oxidation of Aluminum and its Compounds" (submitted for publication - preprints available)
4. D.M. Lindsay and J.L. Gole, J. Chem. Phys. 66, 3886 (1977)
5. S. Rosenwaks, R.E. Steele, and H.P. Broida, J. Chem. Phys. 63, 1963 (1975)
6. J.L. Gole and R.N. Zare, J. Chem. Phys. 57, 5331 (1972)
7. D. Golomb and J.H. Brown, Comb. and Flame 27, 383 (1976)
8. N.W. Rosenberg, D. Golomb, and E.F. Allen, J. Geophys. Res. 68, 3328 (1963)
9. E.R. Johnson, J. Geophys. Res. 70, 1275 (1966)
10. See for example G. Herzberg, "Electronic Spectra of Polyatomic Molecules," D. Van Nostrand Company, New York, New York, 1966. See specifically discussions on page 454-55 and 473-74. See also reference 2 and references therein.
11. N.W. Rosenberg, D. Golomb, and E.F. Allen, J. Geo. Res. 69, 1451 (1964)
12. N.W. Rosenberg, and D. Golomb in "Project Firefly", 1962-63, N.W. Rosenberg, Ed. AFCRL Environmental Research Papers, No. 15, AFCRL-64-364, 1964, Chapter 1.
13. S.A. Flödstrom, R.Z. Rachrach, R.S. Baves, and S.B.M. Hagström, Phys. Rev. Lett. 37, 1282 (1976)

14. For a discussion of the importance of low lying states see
(a) C.J. Chectham and R.F. Barrow in Advances in High Temperature Chemistry (Leroy Eyring Ed.), Academic Press, New York (1967) p. 7
(b) L. Brewer and D.W. Green, High Temp. Sci. 1, 26 (1969)
(c) K.D. Carlson and C.R. Claydon in Advances in High Temperature Chemistry (Leroy Eyring, ed.), Academic Press, New York, (1967). p. 43

15. A very descriptive phrase commonly referred to in energy transfer studies.

16. E.R. Johnson and C.H. Low, Aust. J. Phys. 20, 577 (1967)

17. E.R. Johnson, R.H. Lloyd, C.H. Low, and L.M. Shepard, Aust. J. Phys.

18. The electron jump crossing radius for the aluminum-ozone reaction is $r_c \tilde{=} 4.1\text{Å}$. At this distance formation of the ground electronic state corresponds to formation of the $A^2\Pi$ state with a cross section on the order of 50Å^2. Thus we expect a high photon yield; see reference 4.

19. The reactions must be $\approx 21{,}000\ cm^{-1}$ exothermic. They might include $Al + O_3$, $Al + N_2O$, and $Al + O + M \rightarrow AlO + M$

20. This crucible must be of ultra-high purity. At excessive temperatures one may observe BO_2 emission; however, care was taken to alleviate this problem in the present experiments.

21. The observed AlO, $A^2\Pi_i$ spectrum cannot possibly be assigned to an excited state of AlO_2 analogous to that observed for BO_2 under certain experimental conditions. D.M. Lindsay and J.L. Gole (unpublished) have analyzed the observed BO and BO_2 emissions in these systems, and one can draw analogies to the possible emission from AlO_2.

22. J.K. McDonald and K.K. Innes, J. Mol. Spectros. 32, 501 (1969)

23. J. Schamps, Chem. Phys. 2, 352 (1973)

24. In other words, emission from a given excited state vibrational level will be to several ground state (lower state) levels.

25. The $b'\Sigma_g^+$ state of O_2 lies only 13000 cm^{-1} above the ground $^3\Sigma_g^-$ state and is easily accessible to the reaction exothermicity (4.1 eV) for the aluminum - ozone reaction. In general, one finds that the bond formed possesses much of the reaction exoergicity.

26. (a) J.L. Gole and C.L. Chalek, J. Chem. Phys. 65, 4384 (1976)
(b) C.L. Chalek and J.L. Gole, Chemical Physics 19, (1977)

27. The energy relative to the v" = 0 level of the ground electronic state.

28. The coefficient for the cubic term in the expansion of the potential.

29. The programs used were written by Dr. Brian G. Wicke.

30. G. Herzberg, Spectra of Diatomic Molecules, (Van Nostrand - Reinhold, New York, 1950)

31. M. Yoshimine, A.D. McLean and B. Liu, J. Chem. Phys. 58, 4412 (1973)

32. D.M. Manos and J. Parsons, J. Chem. Phys. 63, 3575, (1975), discuss this approximation.

33. See references 26(a) and (b) and Reference 4 for a further discussion of this point.

34. This is the deviation from the mean.

35. Here we take into account $B^2\Sigma^+ - X^2\Sigma^+$ emission intensity as well as emission from aluminum reaction with possible impurities which lead to aluminum hydration.

36. We normalized to the aluminum atomic lines in Figure 1. See reference 3.

37. D.C. Tyte and R.W. Nicholls, Identification Atlas of Molecular Spectra I: The AlO $A^2\Sigma^+ - X^2\Sigma^+$ Blue-Green System (Univ. of Western Ontario, London, Ontario, 1964)

38. C.L. Chalek and J.L. Gole, J. Chem. Phys. 65, 2845 (1976)

39. Note that this assumes the unperturbed levels are well represented by a Morse potential for levels up to and including v" = 9 for the ground $X^2\Sigma^+$ state and v' = 4 for the $A^2\Pi_i$ state. The constant second differences $\Delta G_{(v+3/2)}$ observed for levels v" = 0 to 8 (Ref. 37) indicates that this is a reasonable assumption. We have employed the experimental data given by Tyte and Nicholls and extended, slightly, the experimental data of McDonald and Innes.

40. H.S. Jarrett, Solid State Phys. 14, 215 (1963); A.J. Stone, Proc. R. Soc. London, Ser. A271, 424 (1963)

41. One might consider the use of a CI wavefunction for the ground state, (reference 31) however, this is beyond the accuracy desired in the present description. It is probable that the spin orbit constant will decrease as the charge distribution for the ground state is represented by a more accurate description, intermediate between Al^+O^- and $Al^{+2}O^{-2}$. The differences between the calculated $A^2\Pi_{1/2} - B^2\Sigma^+_{1/2}$ and $A^2\Pi_{1/2} - X^2\Sigma^+_{1/2}$ interactions can be attributed primarily to the single center nature of the spin orbit interaction and the differences in charge density for the $B^2\Sigma^+$ and $X^2\Sigma^+$ states.

42. The interaction terms on aluminum contribute a negligible factor to $H_{electronic}$. As the charge shifts more to oxygen there will be little effect on the contribution from the aluminum orbitals; however, there will be a marked dimunition of $H_{electronic}$ in equation (18).

43. At 4.1Å, the A state is the ground state while at R < 1.8Å the ground state is the $X^2\Sigma^+$ state. The $A^2\Pi$ state correlates with ground state atoms.

44. The numbers quoted are obtained from the evaluation of the quadratic expansion given by Tyte and Nicholls for the B state, and taken from McDonald and Innes for the A state.

45. Some recent theoretical work suggests that $\omega_e y_e$ should be negative (H. Lefebvre - Brion - private communication)

46. Using standard gas-kinetic collision theory

47. P.J. Dagdigian, H.W. Cruse, and R.N. Zare, J. Chem. Phys. 62, 1824 (1975) and references therein.

48. H.S. Johnson, Gas Phase Reaction Rate Theory (Ronald, New York, 1966)

49. W.H. Flygare, Acc. Chem. Res. 1, 121 (1969)

50. Even though the Coriolis interaction between the $A^2\Pi_{3/2}$ and $B^2\Sigma^+$ states is much smaller than the spin orbit interaction, 500 to 1000 collisions will be quite effective in inducing a transfer from the A to the B state.

51. The possibility of emission from a low lying Al0 $^4\Pi$ state is extremely unlikely. This state, if formed, would be characterized by a radiative lifetime considerably longer than the Al0 $A^2\Pi$ state. Therefore, it is expected to be a much weaker emitter than either the $A^2\Pi$ or $B^2\Sigma^+$ states. Quenching of the $^4\Pi_{3/2}$ or $^4\Pi_{1/2}$ components, if they are formed in the aluminum-ozone reaction, occurs via a mechanism involving coriolis or spin orbit coupling with the $A^2\Pi$ or $B^2\Sigma^+$ states. The formation and subsequent quenching of a $^4\Pi$ state is not indicated by the behavior of the emission spectrum as a function of pressure. Similar arguments hold for the possible emission from an Al0 $^4\Sigma^+$ state. Further discussion is provided in reference 3.

52. Note the discussion in reference 4 page 3892

53. In this regard, it is interesting to note Figure 4, reference 4. It appears that the v' = 0, 1, and 2 levels may be affected slightly by collisional transfer from the A state

54. The characteristics which we have described may also apply to O atom reactions.

Table I: Boltzmann Factors for Various Vibrational Levels v' and Temperatures T_{vib}

v'	ε (cm^{-1})(a)		T_{vib} = 10,000K	T_{vib} = 5000K	T_{vib} = 2500K
7	4867.1	ε/KT_{vib}	0.636	1.271	2.543
		e^{-x}(a)	0.529	0.281	7.863×10^{-2}
10	6828.5	ε/KT_{vib}	0.692	1.784	3.568
		e^{-x}	0.410	0.168	2.821×10^{-2}
16	10527.2	ε/KT_{vib}	1.375	2.750	5.500
		e^{-x}	0.253	6.393×10^{-2}	4.090×10^{-3}
25	15515.0	ε/KT_{vib}	2.027	4.053	8.106
		e^{-x}	0.132	1.737×10^{-2}	3.017×10^{-4}

(a) relative to $\varepsilon(0) = 0$.

(b) $x \equiv \varepsilon/KT$

Figure Captions

Figure 1. Chemiluminscent spectrum from the reaction, Al + O_3, showing the $A^2\Pi_i$-$X^2\Sigma$ (5800-7000$^+$Å), $B^2\Sigma^+$-$X^2\Sigma^+$ (4000-5800Å), and $C^2\Pi_r$ - $X^2\Sigma^+$ (< 3500Å) emission systems. The total (argon) pressure was 5 torr. Spectral resolution is 20Å. The The spectrum is uncorrected for instrument response. Superimposed is the relative response of the RCA 4840 photomultiplier.

Figure 2. Al0 $A^2\Pi_i$ emission from 6000Å to 10,000Å. Below 6000Å the spectrum begins to merge into a featureless emission. The total pressure (argon) was 4 torr. No correction for instrumental response (RCA 7102 photomultiplier) is made. Spectral resolution is ∿ 10Å.

Figure 3. Intensities calculated for the $A^2\Pi_{3/2}$ - $X^2\Sigma^+$ component of the $A^2\Pi_i$ - $X^2\Sigma^+$ system. For the calculation, the upper state vibrational population ($N_{v'}$) and electronic transition moments (R_e) are assumed constant and equal for each vibrational level. Transition (band origin) positions are identified as (v',v"), with sequences Δv = constant marked horizontally. Compare to fig. 2 and see text for explanation.

Figure 4. Calculated population distribution, $N_{v'}$, for the $A^2\Pi_{3/2}$ (—●—) and $A^2\Pi_{1/2}$ (— — x) components of the $A^2\Pi$ state. The peaks at low v' (v' $\leq$ 15) are not considered to be statistically significant. See text for an explanation of the determination and significance of this figure.

Figure 5. Calculated RKR potential curves for the $X^2\Sigma^+$ (——) and $A^2\Pi$(— —) states. Except when specifically noted, the $A^2\Pi$ levels shown are those for the $\Omega = 1/2$ component. Of special interest is the coincidence between the $v' = 4$, $\Omega = 1/2$ and $v'' = 9$, $X^2\Sigma^+$ levels.

Figure 6. Comparison of the "single-collision" (Main figure) and "multiple collision" or relaxed (inset) spectra from the reaction $Al + O_3 \xrightarrow{[Ar]} AlO^*$. The single collision spectrum is dominated by $A^2\Pi$ emission. The multiple collision spectrum clearly shows the effects of efficient collisional transfer from the $A^2\Pi_i$ to the $B^2\Sigma^+$ state. Note that the multiple collision emission from the $B^2\Sigma^+$ state extends to a short wavelength limit $\approx$ 5800Å. See text for discussion.

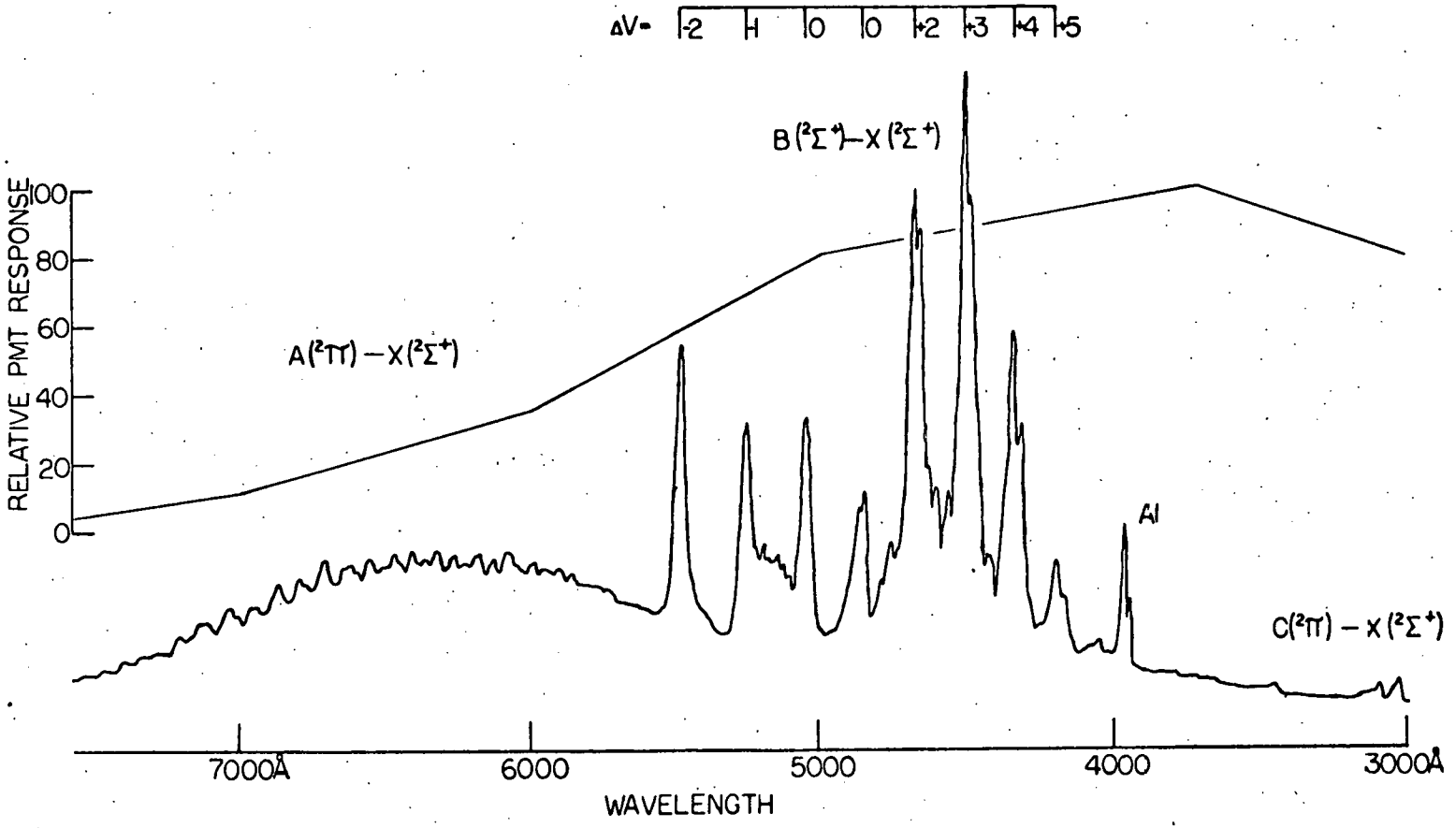
ΔV=
-2
-1
0
0
+2
+3
+4
+5
B(²Σ⁺)–X(²Σ⁺)
A(²Π)–X(²Σ⁺)
Al
C(²Π)–X(²Σ⁺)
RELATIVE PMT RESPONSE
100
80
60
40
20
0
7000Å
6000
5000
4000
3000Å
WAVELENGTH

Figure 1

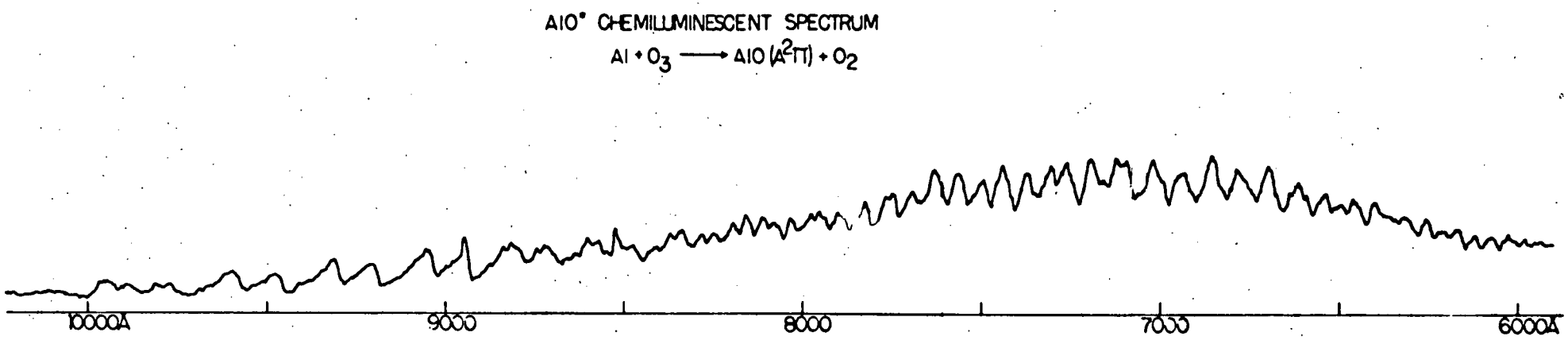
AlO* CHEMILLUMINESCENT SPECTRUM
Al + O3 ⟶ AlO (A²Π) + O2
10000A
9000
8000
7000
6000A

Figure 2

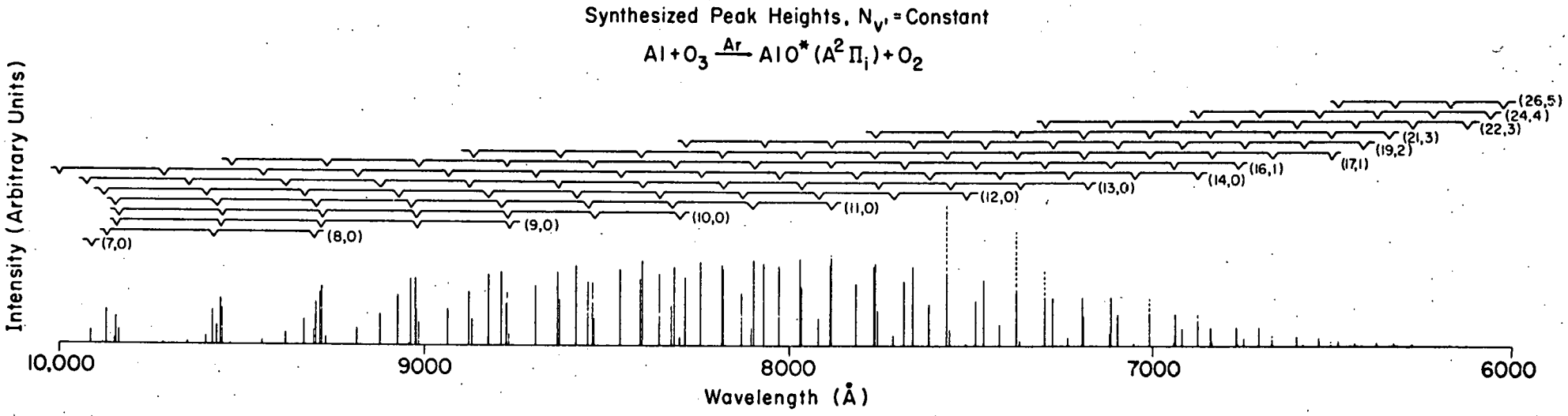
Synthesized Peak Heights, $N_{v'}$ = Constant
$Al + O_3 \xrightarrow{Ar} AlO^*(A^2\Pi_i) + O_2$
Intensity (Arbitrary Units)
(7,0)
(8,0)
(9,0)
(10,0)
(11,0)
(12,0)
(13,0)
(14,0)
(16,1)
(17,1)
(19,2)
(21,3)
(22,3)
(24,4)
(26,5)
10,000
9000
8000
7000
6000
Wavelength (Å)

Figure 3

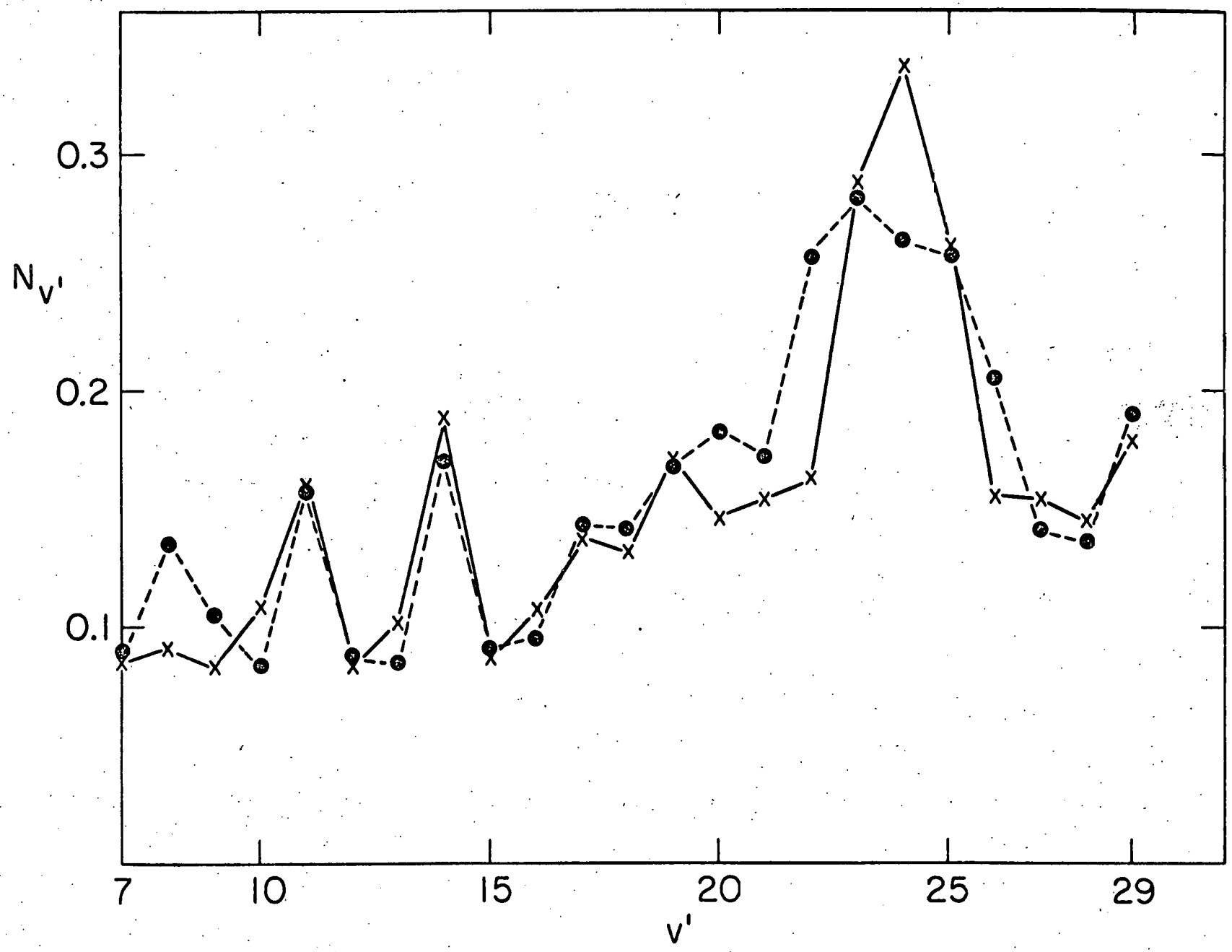

Figure 4

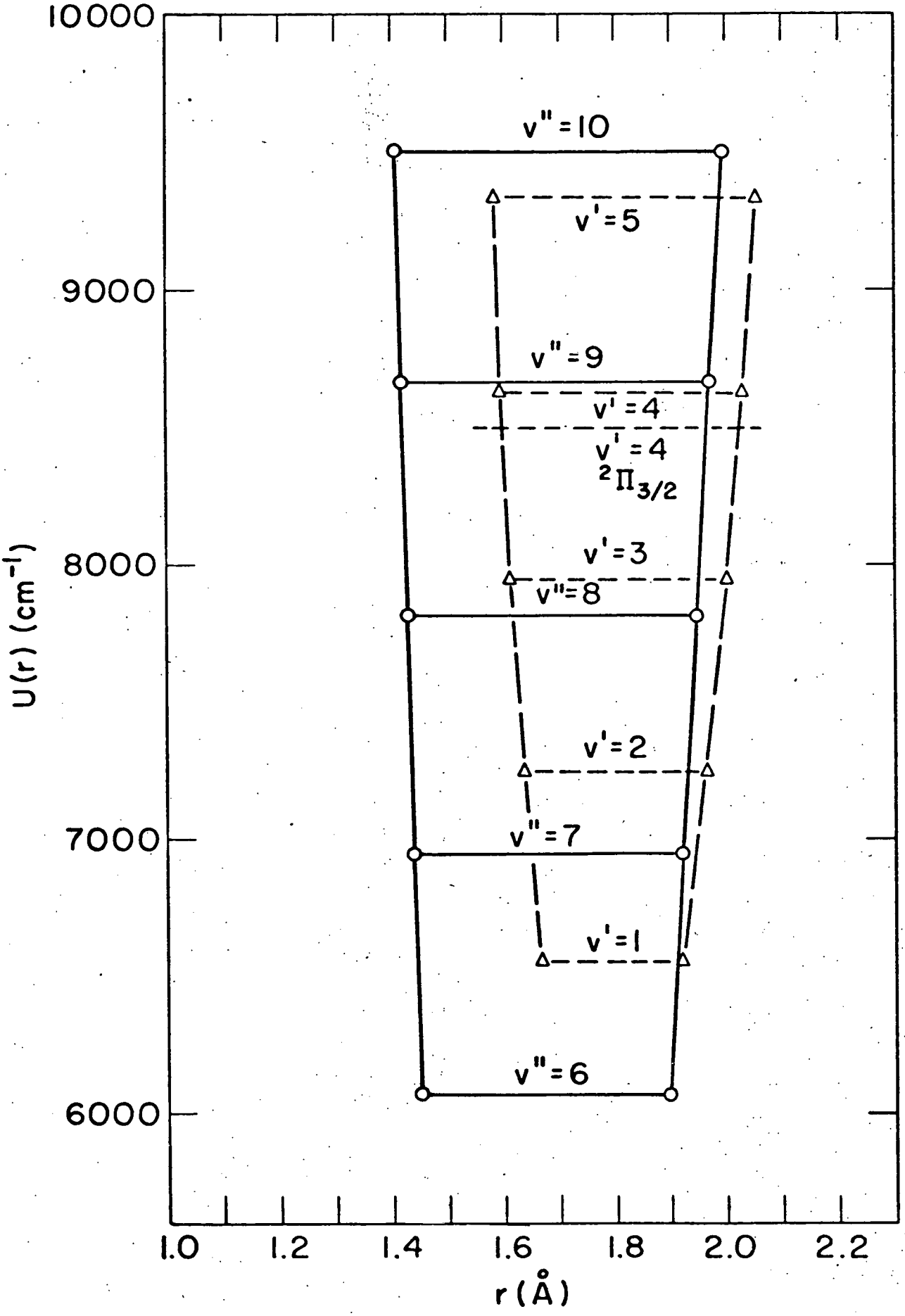
10000
9000
8000
7000
6000
U(r) (cm⁻¹)
v" = 10
v' = 5
v" = 9
v' = 4
v' = 4
²Π3/2
v' = 3
v" = 8
v' = 2
v" = 7
v' = 1
v" = 6
1.0
1.2
1.4
1.6
1.8
2.0
2.2
r (Å)

Figure 5

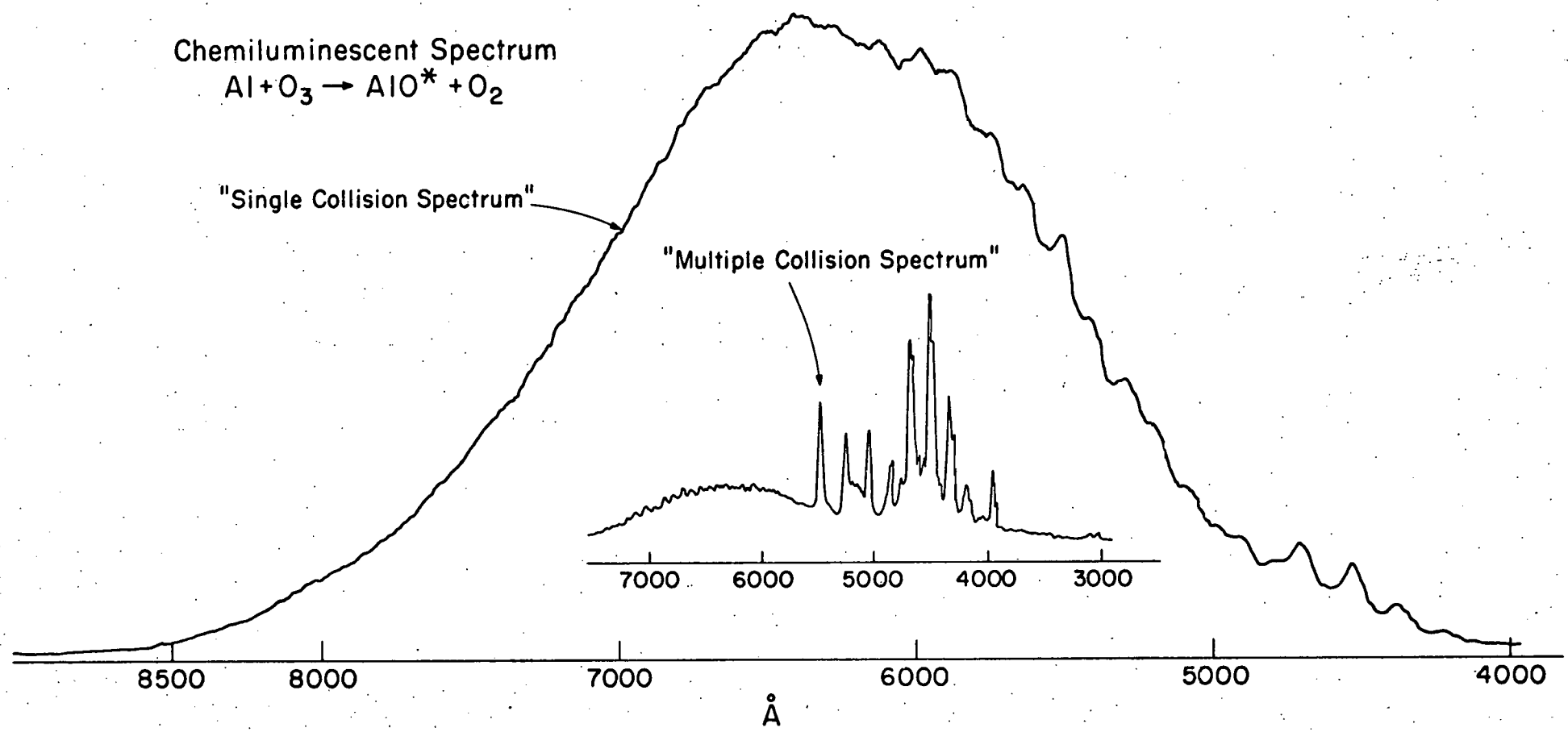
Chemiluminescent Spectrum
Al + O3 → AlO* + O2
"Single Collision Spectrum"
"Multiple Collision Spectrum"
7000
6000
5000
4000
3000
8500
8000
7000
6000
5000
4000
Å

Figure 6